

PACS numbers: 42.50.Ct; 42.50.Gy; 68.65.Hb
DOI: 10.1070/QE2015v045n09ABEH015677

Phase control of group velocity of light in an InGaN/GaN quantum dot nanostructure

H. Jafarzadeh, E. Ahmadi Sangachin, Seyyed Hossein Asadpour

Abstract. **By solving self-consistently Schrödinger–Poisson equations for a carrier in the conduction band of an InGaN/GaN quantum dot, a four-level quantum system is described. It is found that in the presence of terahertz signal radiation, the medium becomes phase dependent, which ensures the phase control of the group velocity of a weak probe pulse from slow to fast light.**

Keywords: *group velocity, relative phase, quantum dot nanostructure.*

1. Introduction

In the past few decades, much attention has been given to quantum optical phenomena based on quantum coherence and interference, such as electromagnetically induced transparency (EIT) [1, 2], lasing without inversion (LWI) [3], four-wave mixing [4, 5], optical solitons [6, 7] and others interesting phenomena [8–15]. In this case, controlling of the group velocity of light leads to both ultraslow and superluminal propagation of light in various systems. Superluminal light propagation is a phenomenon in which the group velocity of an optical pulse in a dispersive medium is greater than of light in vacuum. It has been previously demonstrated that superluminal light propagation originates from the interference of different frequency components of the light pulse. Thus, the coherence of such components plays an important role in superluminal light propagation. On the other hand, atomic coherence due to the coherent laser field has generally been used for controlling the group velocity. It has been shown that in a Raman gain medium with anomalous dispersion, superluminal light propagation is possible via a bi-chromatic driving beam in the regime of electromagnetically induced transparency [16]. In another model proposed by Agarwal et al. [17], it is noted that the group velocity can be controlled by changing the laser field intensity.

Similar phenomena based on the quantum interference and coherence in semiconductor quantum wells (SQWs) and quantum dots (QDs) have also been extensively studied in recent years [18–27], such as gain without population inversion [18], EIT [19], optical bistability/multistability [20–22], Kerr nonlinearity [23], four-wave mixing [24], and others [25–27]. The reason for this is mainly that the phenomena in SQWs and SQDs have many potentially important applications in optoelectronics and solid-state quantum information science. In other words, devices based on intersubband transitions in the SQWs have many inherent advantages over atomic system: electric dipole moments due to the small effective electron mass, great flexibilities in devices' design by choosing the materials and structure dimensions, and high nonlinear optical coefficients. The transition energies and the dipoles as well as the symmetries can also be engineered as desired [25].

In this paper, we propose a novel model for investigating the optical properties of a four-level spherical InGaN QD with a GaN barrier shell which is designed numerically by solving self-consistently Schrödinger and Poisson equations. By controlling the quantum dot size and external voltage, one can design a four level quantum dot with appropriate energy levels which are suitable for interaction with THz signal radiation. In the presence of a THz signal, the medium becomes phase dependent; therefore, we exploit the fact that controlling the relative phase between applied fields can modify the absorption and the dispersion properties of the medium. In this case, the group velocity of the light pulse can be controlled from subluminal to superluminal light values.

2. Model and equations

By solving self-consistently Schrödinger–Poisson equations for a carrier in the conduction band of an InGaN/GaN quantum dot, a four-level quantum system was obtained [27]. The parameters of the problem, such as QD radius and external voltage on it are changed to realise a multilevel nanocrystal. We consider a QD of spherical shape; we start by the following Schrödinger equation and use the method of separation of variables:

$$\frac{\hbar^2}{2m^*}\left[\frac{1}{r^2}\frac{\partial}{\partial r}\left(r^2\frac{\partial}{\partial r}\right)+\frac{1}{r^2\sin\theta}\frac{\partial}{\partial\theta}\left(\sin\theta\frac{\partial}{\partial\theta}\right)+\frac{1}{r^2\sin^2\theta}\frac{\partial^2}{\partial\varphi^2}\right]+V(r). \quad (1)$$

Here, $V(r)$ is the overall potential energy (including a charge-induced potential obtained by solving the Poisson equation, external voltage and conduction band discontinuity for electrons) which depends on r, θ and φ; and m_i^* is the effective mass of the electron [the superscript i refers to a barrier ($i = 1$) or a dot ($i = 0$)]. Based on spherical symmetry, we can assume that $V(r)$ has spherical symmetry.

H. Jafarzadeh, E. Ahmadi Sangachin, Seyyed Hossein Asadpour Sama Technical and Vocational Training College, Islamic Azad University, Tabriz Branch, Tabriz, Iran; e-mail: S.Hosein.Asadpour@gmail.com

Received 22 September 2014; revision received 31 January 2015
Kvantovaya Elektronika **45** (9) 837–843 (2015)
Submitted in English

Thus, the overall potential depends only on the radius r. The total wave function U can be separated into two functions:

$$U(\boldsymbol{R}) = \Psi(r)\,Y(\theta,\varphi). \tag{2}$$

If we substitute U into the Schrödinger equation (1) and introduce the separation constant $\lambda = l(l+1)$, two equations are obtained:

$$\frac{1}{\Psi}\frac{\mathrm{d}}{\mathrm{d}r}\left(r^2\frac{\mathrm{d}}{\mathrm{d}r}\right) + \frac{2m_i^*}{\hbar^2}[E - V(r)] = \lambda, \tag{3}$$

$$-\left[\frac{1}{\sin\theta}\frac{\partial}{\partial\theta}\left(\sin\theta\frac{\partial}{\partial\theta}\right) + \frac{1}{\sin^2\theta}\frac{\partial^2}{\partial\varphi^2}\right]Y = \lambda Y. \tag{4}$$

We will consider the radial differential part of Schrödinger and Poisson equations; thus, the radial part of the Schrödinger equation is written as:

$$-\frac{\hbar^2}{2m_i^*}\left[\frac{\mathrm{d}^2}{\mathrm{d}r^2} + \frac{2}{r}\frac{\mathrm{d}}{\mathrm{d}r} - \frac{l(l+1)}{r^2}\right]\Psi(r) + V_i(r)\,\Psi(r) = E_r\,\Psi(r). \tag{5}$$

Here, l and $\Psi(r)$ are the angular momentum quantum number and the slowly varying envelop, respectively. In order to increase the detection efficiency, the QD is doped and the presence of charge carriers modifies the overlap potential $[V(\boldsymbol{r})]$. Thus, the energy levels and wave functions can be determined precisely by solving the Schrödinger and Poisson equations.

The Poisson equation is written in the form:

$$\nabla^2\phi(r,\theta,\varphi) = -\frac{\rho}{\varepsilon_i^*}\left[\frac{1}{r^2}\frac{\partial}{\partial r}\left(r^2\frac{\partial}{\partial r}\right) + \frac{1}{r^2\sin\theta}\frac{\partial}{\partial\theta}\left(\sin\theta\frac{\partial}{\partial\theta}\right) + \frac{1}{r^2\sin^2\theta}\frac{\partial^2}{\partial\varphi^2}\right]\phi(r,\theta,\varphi) = -\frac{\rho}{\varepsilon_i^*}. \tag{6}$$

After some simplifications, for the radial part of the Poisson equation we obtain:

$$\varepsilon_i^*\left(\frac{\mathrm{d}^2}{\mathrm{d}r^2} + \frac{2}{r}\frac{\mathrm{d}}{\mathrm{d}r}\right)\Phi(r) = -e\left[\overset{+}{N}_{\mathrm{d}}(r) - n(r) - \bar{N}_{\mathrm{a}}(r) + p(r)\right], \tag{7}$$

where N_{d} and N_{a} are the distributions of ionised donors and acceptors, respectively; $n(r)$ and $p(r)$ are the distributions of electrons and holes, respectively; and ε_i^*, $\Phi(r)$ and e are the permittivity of the medium, electrostatic potential and electron charge, respectively. Since we consider intersublevel transitions in the conduction band, we can assume that $N_{\mathrm{a}} = p(r) = 0$. We choose the typical value of N_{d} to be equal to 10^{21} and 10^{24} m^{-3} inside and outside the dot, respectively.

As mentioned above, the overall potential will be modified as follows:

$$V_i(r) = E_{\mathrm{ci}} - e\Phi_i(r), \tag{8}$$

where E_{ci} is the conduction band discontinuity obtained by material composition. The externally applied electric field contributes to the overall potential semi-classically as:

$$V_i(r) = E_{\mathrm{ci}} - e\Phi_i - eV_{\mathrm{ext}}. \tag{9}$$

It is necessary to calculate Φ in the Poisson equation. Thus, we should calculate $n(r)$ with allowed wave functions Ψ and Fermi level E_{F}:

$$n(r) = 2\sum_j\left\{\Psi_j^2(r)\left[1 + \exp\left(\frac{E_j - E_{\mathrm{F}}}{k_{\mathrm{B}}T}\right)\right]^{-1}\right\}, \tag{10}$$

where k_{B} is the Boltzmann constant. Summation over j refers to all allowed wave functions.

In the latter equation, the Fermi level is unknown and can be calculated from the equilibrium condition as:

$$\int_0^\infty N_{\mathrm{d}}^+(r)r^2\mathrm{d}r = \int_0^\infty n(r)r^2\mathrm{d}r. \tag{11}$$

The self-consistent solution of equations (5), (7), (10) yields eigenstates. We repeat this cycle by inserting Φ in the overall potential and calculate the new eigenstates and their corresponding eigenvalues. The Fermi energy level in two successive steps may be chosen as the convergence indicator of this cycle.

In order to evaluate the considerable electric dipole moment elements between QD levels, we should calculate the dipole transition matrix elements:

$$d_{ij} = \langle\Phi_i|r|\Phi_j\rangle. \tag{12}$$

The normalised wave function with related energy eigenvalues are shown in Fig. 1 (Fig. 10 in Ref [27]). Below (Table 3 from [27]), we also present the parameters for calculating wave functions and intrinsic energies in an InGaN/GaN QD.

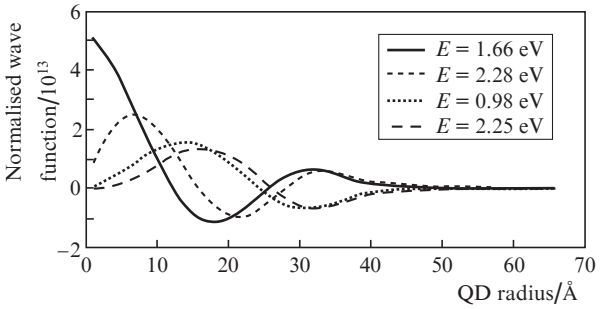

Figure 1. Wave functions of a four-level nanocrystal [the radius of the quantum dot is 35 Å, and the thickness of the shell (barrier) is 30 Å].

QD radius/Å	35
QD barrier/Å	30
Applied external voltage/V	0.5
QD length/Å	65
Number of energy levels obtained	4

Thus, a four-level cascade-type medium coupled by two laser fields and a terahertz driving field is obtained (Fig. 2).

Corresponding to eigenvalues, the wavelengths of the transitions $|1\rangle \leftrightarrow |4\rangle$, $|4\rangle \leftrightarrow |2\rangle$, $|3\rangle \leftrightarrow |2\rangle$ and $|4\rangle \leftrightarrow |3\rangle$ are equal to 0.95, 1.995, 2.097 and 41.2 μm, respectively. A weak tunable probe field with frequency ν_{p} and Rabi frequency $\Omega_{\mathrm{p}} = E_{\mathrm{p}}\wp_{41}/\hbar$ couples the ground state $|1\rangle$ to the exited state $|4\rangle$. Two control fields with frequencies ν_1 and ν_2 and Rabi frequencies $\Omega_1 = E_1\wp_{42}/\hbar$ and $\Omega_2 = E_2\wp_{32}/\hbar$ couple levels $|4\rangle$ with $|2\rangle$ and $|2\rangle$ with $|3\rangle$, while the THz field with frequency ν_3

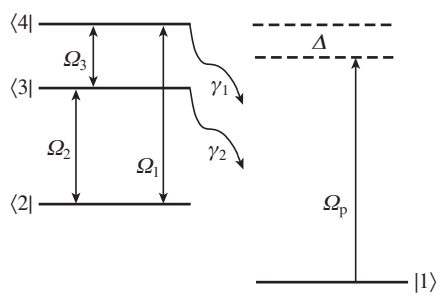

Figure 2. Diagram of a four-level InGaN/GaN quantum dot nanostructure interacting with a terahertz signal and two control fields.

and Rabi frequency $\Omega_3 = E_2\wp_{43}/\hbar$ couples levels $|3\rangle$ and $|4\rangle$, where $\wp_{kl} = \wp_{kl}\boldsymbol{e}_l$ is the intersubband dipole moment for the electron transition between the levels $|k\rangle$ and $|l\rangle$. The total decay rates from levels $|3\rangle$ and $|4\rangle$ to the ground level $|1\rangle$ are denoted by $\gamma_1 = \Gamma_1 + \gamma_1^{\text{dph}}$ and $\gamma_2 = \Gamma_2 + \gamma_2^{\text{dph}}$, where γ_i^{dph} is the dephasing decay rate of the quantum coherence of the transition $|i\rangle \leftrightarrow |j\rangle$, respectively.

The density matrix equations of motion for the system in the rotating frame and under the rotating wave approximation are given by:

$$\begin{aligned}
\frac{\partial\rho_{41}}{\partial t} &= -(\mathrm{i}\Delta + \frac{1}{2}\gamma_1)\rho_{41} + \frac{\mathrm{i}}{2}\Omega_3 \mathrm{e}^{-\mathrm{i}\phi}\rho_{31} \\
&\quad + \frac{\mathrm{i}}{2}\Omega_1\rho_{21} - \frac{\mathrm{i}}{2}\Omega_\mathrm{p}(\rho_{44} - \rho_{11}), \\
\frac{\partial\rho_{31}}{\partial t} &= -(\mathrm{i}\Delta + \frac{1}{2}\gamma_2)\rho_{31} + \frac{\mathrm{i}}{2}\Omega_3 \mathrm{e}^{\mathrm{i}\phi}\rho_{41} \\
&\quad + \frac{\mathrm{i}}{2}\Omega_2\rho_{21} - \frac{\mathrm{i}}{2}\Omega_\mathrm{p}\rho_{34}, \\
\frac{\partial\rho_{21}}{\partial t} &= -\mathrm{i}\Delta\rho_{21} + \frac{\mathrm{i}}{2}\Omega_1\rho_{41} + \frac{\mathrm{i}}{2}\Omega_2\rho_{31} - \frac{\mathrm{i}}{2}\Omega_\mathrm{p}\rho_{24}, \\
\frac{\partial\rho_{43}}{\partial t} &= -[\mathrm{i}\Delta_1 + \frac{1}{2}(\gamma_1 + \gamma_2)]\rho_{43} - \frac{\mathrm{i}}{2}\Omega_3 \mathrm{e}^{-\mathrm{i}\phi}(\rho_{44} - \rho_{33}) \\
&\quad + \frac{\mathrm{i}}{2}\Omega_1\rho_{23} - \frac{\mathrm{i}}{2}\Omega_2\rho_{42} + \frac{\mathrm{i}}{2}\Omega_\mathrm{p}\rho_{13}, \\
\frac{\partial\rho_{42}}{\partial t} &= -(\mathrm{i}\Delta_2 + \frac{1}{2}\gamma_1)\rho_{42} - \frac{\mathrm{i}}{2}\Omega_1(\rho_{44} - \rho_{22}) \\
&\quad - \frac{\mathrm{i}}{2}\Omega_2\rho_{43} + \frac{\mathrm{i}}{2}\Omega_3 \mathrm{e}^{-\mathrm{i}\phi}\rho_{32} + \frac{\mathrm{i}}{2}\Omega_\mathrm{p}\rho_{12}, \qquad (13) \\
\frac{\partial\rho_{32}}{\partial t} &= -(\mathrm{i}\Delta_3 + \frac{1}{2}\gamma_2)\rho_{32} - \frac{\mathrm{i}}{2}\Omega_2(\rho_{33} - \rho_{22}) \\
&\quad - \frac{\mathrm{i}}{2}\Omega_1\rho_{34} + \frac{\mathrm{i}}{2}\Omega_3 \mathrm{e}^{\mathrm{i}\phi}\rho_{42}, \\
\frac{\partial\rho_{33}}{\partial t} &= \frac{\mathrm{i}}{2}\Omega_2(\rho_{23} - \rho_{32}) + \frac{\mathrm{i}}{2}\Omega_3 \mathrm{e}^{\mathrm{i}\phi}\rho_{43} \\
&\quad - \frac{\mathrm{i}}{2}\Omega_3 \mathrm{e}^{-\mathrm{i}\phi}\rho_{34} - \gamma_2\rho_{33}, \\
\frac{\partial\rho_{22}}{\partial t} &= \frac{\mathrm{i}}{2}\Omega_2(\rho_{32} - \rho_{23}) + \frac{\mathrm{i}}{2}\Omega_1(\rho_{42} - \rho_{24}), \\
\frac{\partial\rho_{11}}{\partial t} &= \frac{\mathrm{i}}{2}\Omega_\mathrm{p}(\rho_{41} - \rho_{14}) + \gamma_1\rho_{44} + \gamma_2\rho_{33}, \\
\rho_{11} + \rho_{22} + \rho_{33} + \rho_{44} &= 1.
\end{aligned}$$

Here, $\Delta = \omega_{41} - \nu_\mathrm{p}$ is the frequency detuning of the probe field; ω_{41} is the frequency deference between levels $|4\rangle$ and $|1\rangle$; and ν_p is the frequency of the probe field. We consider the resonance condition, when the frequency detuning of the other laser fields are set to be zero, i.e., $\Delta_1 = \Delta_2 = \Delta_3 = 0$. Note that the three driving fields form a closed loop, so that the phase can be inserted into any one of them. In other words, if all the fields were phase dependent, only the collective phase would be important and no individual phase-dependent term would play any role. The collective phase is here defined as $\phi = \varphi_3 + \varphi_2 - \varphi_1$. Therefore, without the loss of generality, Ω_1 and Ω_2 can be considered real, while Ω_3 carries the phase, i.e., $\Omega_3 = |\Omega_3|\mathrm{e}^{-\mathrm{i}\phi}$.

Now, we continue to treat the numerical results in order to obtain the steady state behavior of the probe field absorption and dispersion as well as the group velocity when the driving fields are switched on. It is assumed that the system is initially in the ground state, so that $\rho_{11}(0) = 1, \rho_{ij}(0) = 0$ $(i,j = 1,2,3,4)$. Furthermore, we assume that the intensity of the probe field is sufficiently weaker than the driving fields, such that all the atoms remain in the ground state. Therefore, the system of equations (13) can be written in the form

$$\dot{R} = -MR + C, \qquad (14)$$

where R and C are the column vectors and M is a matrix as given bellow:

$$R = (\rho_{41} \;\; \rho_{31} \;\; \rho_{21})^\mathrm{T}, \qquad (15)$$

$$C = \left(\frac{\mathrm{i}}{2}\Omega_\mathrm{p} \;\; 0 \;\; 0\right)^\mathrm{T}, \qquad (16)$$

$$M = \begin{pmatrix} \mathrm{i}\Delta + \frac{1}{2}\gamma_1 & -\frac{\mathrm{i}}{2}|\Omega_3|\,\mathrm{e}^{-\mathrm{i}\phi} & -\frac{\mathrm{i}}{2}\Omega_1 \\ -\frac{\mathrm{i}}{2}|\Omega_3|\,\mathrm{e}^{\mathrm{i}\phi} & \mathrm{i}\Delta + \frac{1}{2}\gamma_2 & -\frac{\mathrm{i}}{2}\Omega_2 \\ -\frac{\mathrm{i}}{2}\Omega_1 & -\frac{\mathrm{i}}{2}\Omega_2 & \mathrm{i}\Delta \end{pmatrix}. \qquad (17)$$

The formal solution of this equation has the form:

$$R(t) = \int_{-\infty}^{t} \exp[-M(t-t')]\,C\mathrm{d}t' = M^{-1}C. \qquad (18)$$

We use equation (18) to obtain the solution for ρ_{41}:

$$\rho_{41} = \frac{1}{Y\hbar}(\Omega_2^2 - 4\Delta^2 + \mathrm{i}2\gamma_2\Delta)E_\mathrm{p}\mu_{41}, \qquad (19)$$

where

$$\begin{aligned}
Y &= A + \mathrm{i}B, \\
A &= -8\Delta^3 + 2\Delta(\Omega_1^2 + \Omega_2^2 + \Omega_3^2) \\
&\quad + 2\gamma_1\gamma_2\Delta + \Omega_1\Omega_2\Omega_3(\mathrm{e}^{\mathrm{i}\phi} + \mathrm{e}^{-\mathrm{i}\phi}), \qquad (20) \\
B &= 4\Delta^2(\gamma_1 + \gamma_2) - (\gamma_1\Omega_2^2 + \gamma_2\Omega_1^2).
\end{aligned}$$

Note now that the susceptibility can be written as:

$$\chi = \frac{2N|\mu_{41}|^2}{\varepsilon_0}\frac{\Omega_2^2 - 4\Delta^2 + i2\gamma_2\Delta}{Y\hbar}, \tag{21}$$

where N is the atom number density in the medium. Separating the real and imaginary parts $\chi = \chi' + i\chi''$, we obtain

$$\chi' = \frac{2N|\mu_{41}|^2}{\varepsilon_0\hbar Z}[(\Omega_2^2 - 4\Delta^2)A + 2\gamma_2\Delta B], \tag{22}$$

$$\chi'' = \frac{2N|\mu_{41}|^2}{\varepsilon_0\hbar Z}[2\gamma_2\Delta A - (\Omega_2^2 - 4\Delta^2)B], \tag{23}$$

where $Z = YY'$. It is imperative to point out that the phase enters the susceptibility expression only through quantities A and Y. Moreover, the phase dependence of Y is expressed only through A. Thus, this phase factor could very well have emerged from either of the three driving fields. Moreover, if all the fields had phase dependence, only the collective phase would be important and no individual phase-dependent terms would occur. From equations (22) and (23) we can find that under the resonance condition for the probe field, the parameter Ω_2 is important for calculating absorption, dispersion and group velocity in such a system. If $\Omega_2 = 0$, the absorption and dispersion will vanish. Thus, the existence of Ω_2 is a necessary condition to control the optical behavior of the group velocity, while the existence of Ω_3 (terahertz signal) is a necessary condition to make the system phase dependent. Therefore, for $\Omega_3 = 0$, the phase dependence of the medium will disappear.

3. Results and discussion

In terms of this model, we can also determine the group velocity of light according to [28]

$$v_{gr} \equiv \frac{d\omega}{dk} = \frac{c}{n + \omega(dn/d\omega)}, \tag{24}$$

where $n = 1 + 2\pi\chi$; then,

$$\frac{c}{v_{gr}} = 1 + 2\pi\,\mathrm{Re}\,\chi(\omega) + 2\pi\omega\,\mathrm{Re}\frac{d\chi}{d\omega}. \tag{25}$$

It is found that from Eqn (25), when $\mathrm{Re}\chi(\omega)$ is zero and the dispersion is positive and strongly depends on the frequency

$$\frac{c}{v_{gr}} - 1 = 2\pi\omega\,\mathrm{Re}\frac{d\chi}{d\omega}. \tag{26}$$

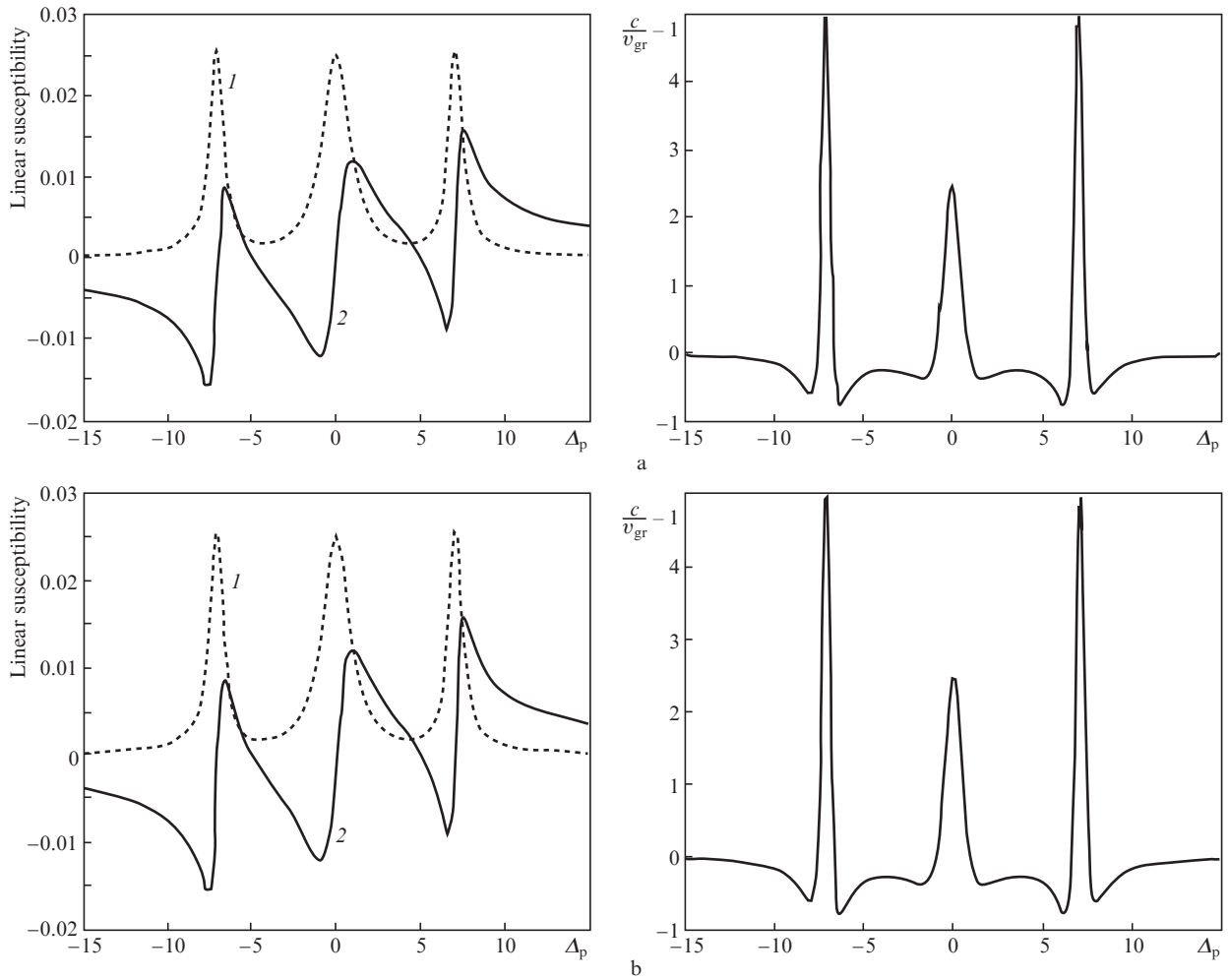

Figure 3. Linear susceptibility of the probe pulse [hereinafter, curve (*1*) shows absorption and curve (*2*) – dispersion] and group velocity vs. probe field detuning in the absence of a terahertz signal field at $\Omega_1 = \Omega_2 = 10$, $\Omega_3 = 0$ and $\gamma_1 = \gamma_2 = 2\gamma$ in the case of ϕ = (a) 0 and (b) π.

It means that the group velocity shows continuous tunability over a wide range of values ranging from subluminal to superluminal with changing the phase of one of the control fields, other parameters being kept constant. Figure 3 shows the dependence of the susceptibility and ratio of the velocities of light in vacuum and medium for a weak probe light field in

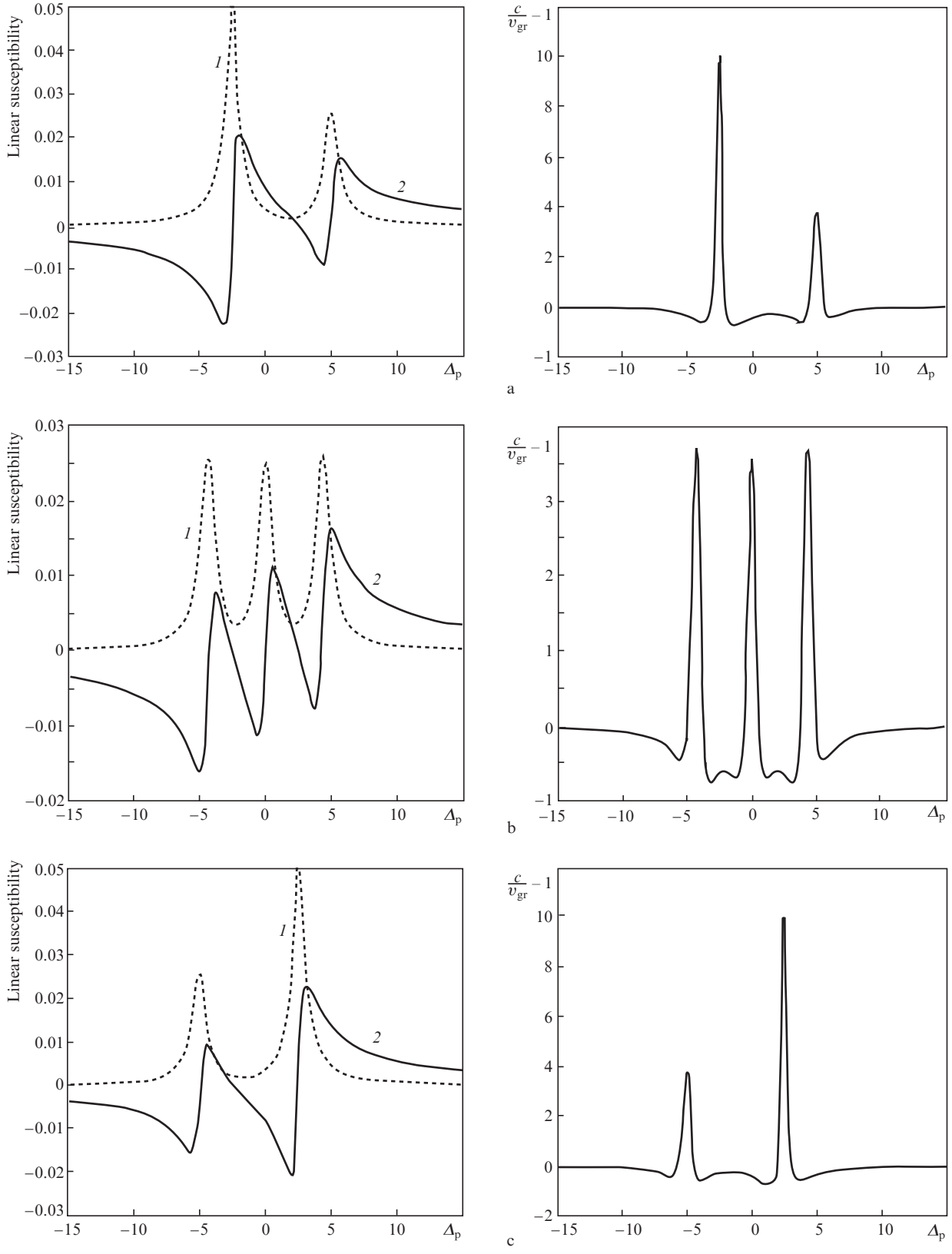

Figure 4. Linear susceptibility of the probe pulse and group velocity vs. probe field detuning in the presence of a terahertz signal field at $\Omega_1 = \Omega_2 = \Omega_3 = 5$, and $\gamma_1 = \gamma_2 = 2\gamma$ in the case of ϕ = (a) 0, (b) $\pi/2$ and (c) π.

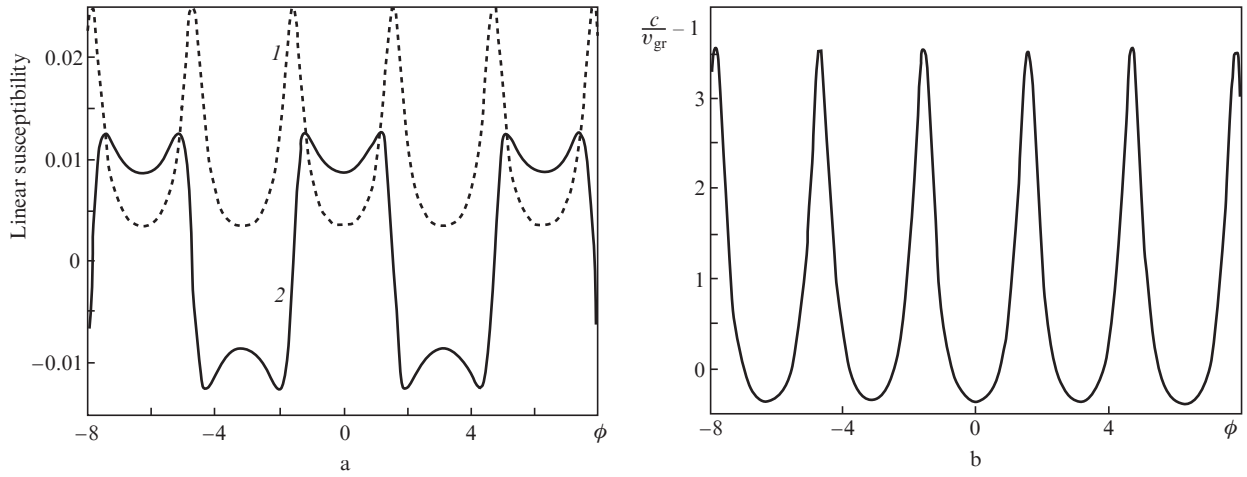

Figure 5. Variation of (a) susceptibility and (b) group velocity as a function of ϕ at $\Omega_1 = \Omega_2 = \Omega_3 = 5$ and $\gamma_1 = \gamma_2 = 2\gamma$.

the absence of the terahertz field on the detuning of the probe field from the resonance at different relative phases of the control fields. One can see that in the absence of a terahertz signal field the medium is not phase dependent. Therefore, the sign of the slope of the dispersion does not change with the relative phase. In this case, the group velocity of the probe pulse cannot switch from subluminal to superluminal.

However, in the presence of a terahertz signal field (Fig. 4), this dependence appears and we observe a change in the sign of the slope of the dispersion with the phase giving rise to 'switching' of the group velocity of the probe pulse from superluminal to subluminal. The dependences of the susceptibility and the ratio of the velocities of light in vacuum and a medium for a weak probe light pulse on the relative phase of control fields are shown in Fig. 5. It can be seen that the absorption, dispersion and group velocity of the probe pulse can be changed continuously by varying the relative phase. Therefore, superluminal and subluminal light propa-

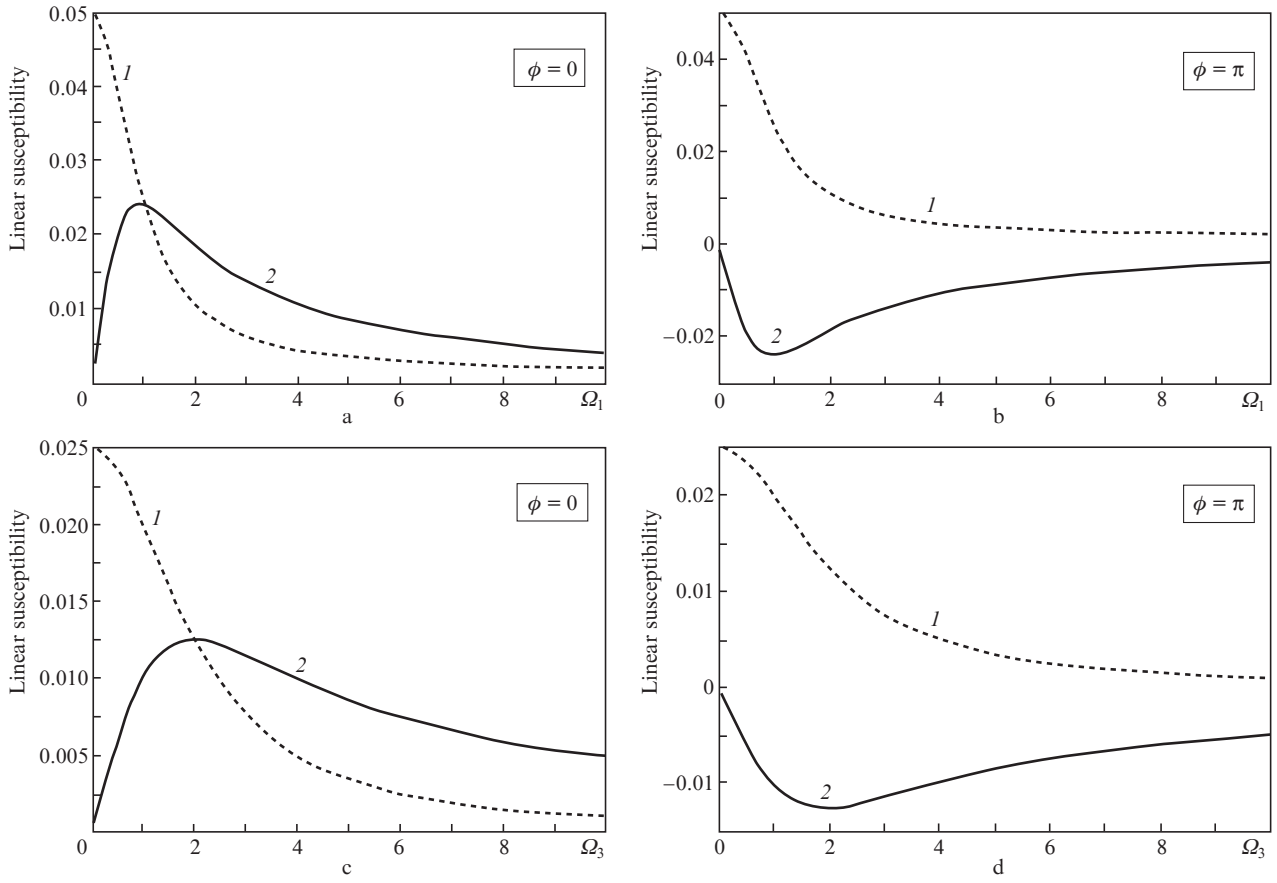

Figure 6. Intensity tuning of susceptibility variation vs. (a, b) Ω_1 and (c, d) Ω_3. Other parameters are the same as in Fig. 5.

gation is possible when changing the relative phase of the applied fields. In this case, the superluminal light propagation is accompanied by reduced absorption which means that the pulse is not attenuated considerably as it passes through the medium. Therefore, our model shows the phase control of the group velocity is possible.

Figure 6 shows the dependences of absorption and dispersion properties of weak probe light on Ω_1 and Ω_3 at $\phi = 0$ and π. One can see that a wide range of tunability and switching from subluminal to superluminal group velocities can be provided.

4. Conclusions

Thus, we have discussed the effect of the phase and amplitude of the driving fields on absorption, dispersion and propagation properties of a probe field applied to an InGaN/GaN quantum dot nanostructure. We have calculated the quantum dot nanostructure numerically by solving self-consistently Schrödinger and Poisson equations. By controlling the size of the quantum dot and the external voltage, we have obtained a four level quantum dot with appropriate energy levels which can be suitable for controlling the superluminal and subluminal light propagation by a terahertz signal field. We have shown that in the presence of a terahertz signal field, the medium becomes phase dependent and therefore the group velocity of the probe field can be tuned in a wide range by changing the phase of the terahertz field. The group velocity can also be switched from subluminal to superluminal through a continuous change of the phase.

References

1. Wu Y., Yang X. *Phys. Rev A*, **71**, 053806 (2005).
2. Harris S.E. *Phys. Today*, **50** (7), 36 (1997).
3. Zhao Y., Huang D., Wu C. *J. Opt. Soc. Am. B: Opt. Phys.*, **13**, 1614 (1996).
4. Wu Y., Yang X. *Phys. Rev. A*, **70**, 053818 (2004).
5. Wu Y., Yang X. *Phys. Rev. B*, **76**, 054425 (2007).
6. Si L.G., Yang W.X., Lou X.Y., Hao X.Y., Yang X. *Phys. Rev. A*, **82**, 013836 (2010).
7. Yang W.X., Hou J.M., Lin Y.Y., Lee R.K. *Phys. Rev. A*, **79**, 033825 (2009).
8. Li J.H., Lou X.Y., Luo J.M., Huang Q.J. *Phys. Rev. A*, **74**, 035801 (2006).
9. Wang Z., Yu B. *Laser Phys. Lett.*, **11**, 035201 (2014).
10. Si L.G., Yang W.X., Yang X. *J. Opt. Soc. Am. B*, **26**, 478 (2009).
11. Asadpour S.H., Hamedi H.R., Rahimpour Soleimani H. *J. Mod. Opt.*, **60**, 659 (2010).
12. Wu Y., Deng L. *Phys. Rev. Lett.*, **93**, 143904 (2004).
13. Asadpour S.H., Eslami-Majd A. *J. Lumin.*, **132**, 1477 (2012).
14. Wu Y.,Yang X. *Appl. Phys. Lett.*, **91**, 094104 (2007).
15. Li J.H., Yu R., Hao X., Zheng A., Yang X. *Opt. Commun.*, **282**, 4384 (2009).
16. Wang L.J., Kuzmich A., Dogariu A. *Nature (London)*, **406**, 277 (2000).
17. Agarwal G.S., Dey T.N., Menon S. *Phys. Rev. A*, **64**, 053809 (2001).
18. Sadeghi S.M., Leffler S.R., Meyer J. *Opt. Commun.*, **151**, 173 (1998).
19. Sadeghi S.M., Leffler S.R., Meyer J. *Phys. Rev. B: Condens. Matter.*, **59**, 15388 (1999).
20. Li J.H. *Phys. Rev. B*, **75**, 155329 (2007).
21. Wang Z., Yu B. *J. Opt. Soc. Am. B*, **30**, 2915 (2013).
22. Asadpour S.H., Jaberi M., Rahimpour Soleimani H. *J. Opt. Soc. B*, **30**, 1815 (2013).
23. Asadpour S.H., Hamedi H.R., Eslami Majd A., Sahrai M. *Phys. E*, **44**, 464 (2011).
24. Wu Y. *J. Appl. Phys.*, **103**, 104903 (2008).
25. Yang W.X., Chen A.X., Lee R.K., Wu Y. *Phys. Rev. A*, **84**, 013835 (2011).
26. Asadpour S.H., Rahimpour Soleimani H. *Opt. Commun.*, **315**, 347 (2014).
27. Asadpour S.H., Golsanamlou Z., Rahimpour Soleimani H. *Phys. E*, **54**, 45 (2013).
28. Boyd R.W., Gauthier D.J. *Progr. Opt.*, **43**, 497 (2002).